EFFECT OF AGING OF PET FIBRE ON THE MECHANICAL PROPERTIES OF PET FIBRE REINFORCED CEMENT COMPOSITE

VLADIMÍR MACHOVIČ*,***, JANA ANDERTOVÁ*, LUBOMÍR KOPECKÝ**, MARTIN ČERNÝ***,
LENKA BORECKÁ***, OLDŘICH PŘIBYL***, FRANTIŠEK KOLÁŘ***, JAROSLAVA SVÍTILOVÁ***

*Institute of Chemical Technology Prague, Technická 5, 166 28, Prague, Czech Republic
**Czech Technical University in Prague, Faculty of Civil Engineering, Thákurova 7, 166 29 Prague, Czech Republic
***Institute of Rock Structure and Mechanics, Academy of Sciences of the Czech Republic,
V Holešovičkách 41, 182 09 Prague, Czech Republic

E-mail: machoviv@vscht.cz

Poly(ethylene terephthalate) (PET) fibres have been used as a dispersed micro-reinforcement in a cementitious matrix. The micro-reinforcement in the fibre reinforced concrete absorbs tensile strain and prevents formation of microcracks originating from concrete shrinkage. The present work has been aimed at studying the effects of aging PET fibres by alkali hydrolysis and temperature cycles on the compressive and flexural strength of the PET-cement composite. Using differential scanning calorimetry, infrared spectroscopy and water vapour sorption, chemical changes of PET fibres after their degradation have been characterized together with their effect on mechanical properties of the fibres and the resulting PET-cement composite. It has been found that the flexural strength of the composite has been increased by alkali hydrolysis of PET fibres in sodium hydroxide.

INTRODUCTION

The increasing amount of poly(ethylene terephthalate) (PET) waste is a worldwide problem which has induced requirements for its recycling and reusing. That is why papers focused on utilization of PET fibres as micro-reinforcement for fibre reinforced concretes have been published recently [1,2]. Quality of the micro-reinforcement depends on many factors such as properties of cementitious matrix, fibre geometry, its surface, size, quantity, and rheological parameters.

Concrete represents a three-phase composite consisting of the cementitious matrix, fibres (and other aggregates), and the interfacial transition zone (ITZ). Microstructure of the ITZ between a fibre and the matrix differs from the bulk cement paste and is a critical point determining the concrete strength.

Addition of natural [3-6], steel [7], glass [8], polymeric [9-12], and carbonaceous fibres [13] and carbonaceous nanotubes [14] to mortars and concretes can modify their parameters such as tensile strength, elastic modulus and strength. For improvement of the cement composite properties by fibre addition, the fibres must be easily dispersed within the mixture, have suitable mechanical properties, and finally have persistent properties in the highly alkaline matrix. Silva et al. [1] studied using polyester fibres in the Portland cement matrix and have found that these fibres were loosing their

strength. Aging of PET fibres in the alkaline environment of a cementitious matrix, where calcium hydroxide concentrates in the ITZ and pH reaches a value of about 12, was simulated by modifying the fibres in saturated calcium hydroxide solution at an increased temperature. Recycled PET fibres reacted with calcium hydroxide forming terephthalates on the fibre surface. After degradation, the tested PET fibres in the amount of 0.4 - 0.8 vol% had no significant effect on the compressive and flexural strength of mortars. Elastic modulus of the mortars was not affected by the PET fibres quantity. Firmness of the mortars expressed by the flexural strength was increased by the PET fibres addition.

Japanese authors [2] used the recycled PET fibres from waste PET bottles as a micro-reinforcement in concrete. Good mixability of the fibres and concrete has been found at the PET fibre concentration of 3 wt.%. It has been shown that PET fibres are alkali resistant and their price is comparable to steel fibres. At present, the fibres are used in Japan in tunnel construction.

The present work has studied chemical and thermal degradation of PET fibres within a cementitious matrix. The chemical degradation has been simulated by alkali hydrolysis of the PET fibres in NaOH solution or a saturated $Ca(OH)_2$ solution, which as a product of cement hydration concentrates in the transition zone surrounding the micro-reinforcement. Thermal aging of the PET fibres was realized by temperature cycles in

a thermostated chamber under constant humidity. This way, the chemical degradation of the fibres during hydration of the cementitious matrix under varying weathering temperatures has been simulated, and simultaneously the effect of changes in the surface quality and adhesion of the fibres to concrete mixture in dependence on mechanical properties of the PET-cement composite.

EXPERIMENTAL

Samples were prepared only from a cementitious matrix without sand or gravel aggregate to enable detection of minimum effect of the modified PET fibres on the composite mechanical properties. The samples were prepared by mixing an ordinary Portland cement with water (w:c = 0.4) and the PET fibres (2 wt.%) with a length of 10 mm. The fibre is a discontinual technical polyester fibre produced by SLOVKORD, Inc., Senica, Slovakia. It has a circular section (see Figure 1) with a diameter 26.7 μm, and was provided as a strand containing 195 monofilaments.

Alkali hydrolysis of the PET fibres was achieved by 1 M NaOH solution or saturated $Ca(OH)_2$ solution. The fibres were soaked in the solution, initially heated to 90°C at a heating rate of 10°C per minute, and then left at an ambient temperature for three days. The fibres were washed in distilled water after hydrolysis. The PET fibre samples treated by alkali hydrolysis with $Ca(OH)_2$ and NaOH have been denoted as PET AHCa and PET AHNa, respectively.

Laboratory degradation of PET fibres simulating aging by weathering were carried out in a thermostated chamber Klimaprüfkammer 3533/15, Feutron Klimasimulation GmbH, Germany, at a constant relative humidity of 70% in ten cycles under following aging conditions: sample PET A1 (25°C) - (50°C), sample PET A2: (-40°C) - (25°C), sample PET A3: (-40°C) - (50°C), sample PET A4: (-40°C) - (180°C). All samples gained yellowish colour after degradation.

Infrared spectra were acquired using a Nicolet Nexus FTIR spectrometer equipped with a Specac Golden Gate ATR accessory. The latter was fitted with a diamond crystal, and operated with single reflection optics at an interaction angle of 45° and a probe area of 0.6 mm diameter; the sampling depth (at 1000 cm⁻¹) was calculated to be approximately 3 μm. The spectra were recorded over the range 4000-650 cm⁻¹, with a resolution of 4 cm⁻¹, and averaged over 32 scans. Subsequent manipulation was carried out with Omnic 7.3 software.

The differential scanning calorimetry (DSC) measurements were performed on a Perkin Elmer DSC 7 calorimeter at a heating rate of 10°C/min. Each thermogram was recorded from 25 to 350°C. From the meas-

ured heat of fusion (ΔH_{exp}), an apparent crystallinity degree, %C_{DSC}, was determined according to the equation %$C_{DSC} = 100 \ \Delta H_{exp}/\Delta H°$, where $\Delta H°$ is the heat of fusion of an ideal PET crystal, for which a value of 117.7 J/g was considered.

To study water vapour sorption onto PET fibres, a gravimetric analyzer IGA-02 by Hiden Analytical Ltd., Warrington, UK was used. Ultrahigh vacuum system of the instrument enables to measure adsorption and desorption with a high precision. The instrument is fully thermostabilized with a deviation of 0.2 K. Weight microbalance has a long-term stability 1 μg with a deviation of 0.2 μg. Prior to measuring, the fibre samples were degassed at a pressure < 10⁻⁵ Pa and temperature 353 K. Adsorption was measured at a constant temperature of 298 K. With respect to the microporous texture of the PET fibres studied, measurements of the CO_2 sorption isotherm were done for determination of the microporous surface and micropore distribution. The IGA-02 gravimetric analyzer was used as well for the sorption measurements. Instrument setting and measurement conditions were same as at water vapour sorption except for the sorption pressure. The CO_2 sorption was measured within a pressure range of 0-0.1 MPa.

Microstructure and microtexture of the PET fibre surface were studied by a scanning electron microscope XL30 ESEM-TMP (FEI Philips) with an EDAX microanalyzer, providing high quality pictures in both high and low modes regimes as well as in the environmental (so called ESEM) mode.

Mechanical properties were measured using an Inspekt 100 testing machine. Determination of the tensile strength of a bundle was done with a bundle fixed at both ends by belting a cam at a length of 500 mm at a feed speed of 9 mm/min.

The three-point bending test was done with a support distance of 80 mm (sample size 20×20×100 mm³) and at a feed speed of 0.2 mm/min. The experiments were car-
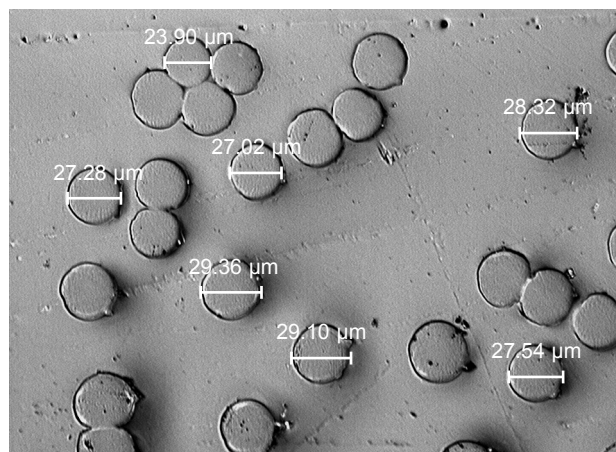

Figure 1. Micrograph of a PET fibre polished section.

ried out at an ambient temperature after 40 days of the composite hydration. For the pressure test, feed speed of 0.05 mm/min was used (sample size 20×20×20 mm). The mechanical experiments were carried out with multiple samples.

Porosimetric determinations were carried out using a high-pressure mercury porosimeter PASCAL 240 by Thermo Electron. The measurements were done within a pressure range of 0.1-200 MPa with a precision better than 0.2 %. According to Washburn's equation, the pressure range corresponds to a pore size ranging from 3.7 to 7500 nm.

RESULTS AND DISCUSSION

Characterization of PET fibres

Poly(ethylene terephthalate) (PET) is one of the most versatile polymers used in films and fibres thanks to its high glass transition temperature (T_g) and slow crystallization rate, which enable controlling its final morphology by various methods. PET belongs to oriented semicrystalline polymers containing both crystalline and amorphous fractions. These polymers can be well characterized by T_g, melting temperature (T_m), and degree of crystallization (W_K). Based on these parameters, deformation behaviour of PET can be predicted.

The differential scanning calorimetry

The structural part of the chain –O–CH$_2$–CH$_2$–O– in a PET molecule can be arranged in the form of either *gauche* or *trans* conformation isomers formed by inner rotation around a C–C bond [18]. The *trans* conformation isomers appear mainly in the crystalline part of the polymer. They have the lowest internal energy and closest arrangement, whereas the *gauche* isomers form mainly amorphous zones of the polymeric chains.

The content of the *trans* conformation isomers in the crystalline fraction, so called degree of crystallization, has been determined by DSC. The values deter-

mined are presented in Table 1 together with the minimum and maximum temperature of degradation of the original PET fibre samples. All samples, except for a fibre sample alkali hydrolyzed by sodium hydroxide, show a higher degree of crystallization compared to the original fibres. It is evident from the table that the fibres subject to the minimum temperature of -40°C have the highest degree of crystallization.

In the DSC thermograms, several endothermic peaks appear within a region near the melting point (see Figure 2 and Table 1). In the case of PET fibres, a lower temperature peak is usually assigned to crystallites of a smaller size, characterized by a lower degree of perfection [16]. For the original PET fibre sample, two peaks appear at the temperatures of 251 and 259°C. For the samples aged by temperature cycles, except for the A3 sample, only one peak is observed. The sample hydrolyzed by sodium hydroxide is characterized by a complex thermogram, in which five peaks within the melting region between 252 and 266°C can be found.
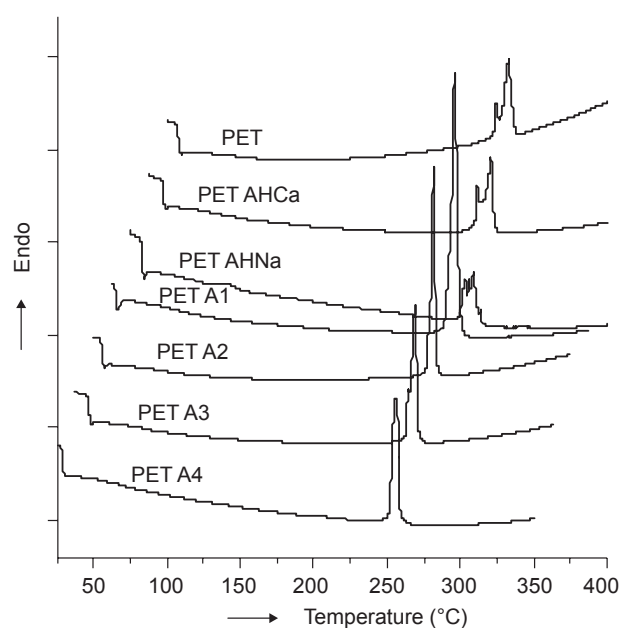

Figure 2. DSC thermograms of the original and modified PET fibres.

Table 1. Content of the crystalline trans conformation isomers, minimum and maximum temperatures used for sample degradation, and melting temperatures observed in DSC thermograms of the original and modified PET fibres.

Sample	crystalline *trans* (%)	T_{min} (°C)	T_{max} (°C)	$T1$ (°C)	$T2$ (°C)	$T3$ (°C)	$T4$ (°C)	$T5$ (°C)
PET	43.54	25	25	251	–	259	–	–
PET AHCa	46.32	25	90	250	–	259		–
PET AHNa	41.97	25	90	252	256	258	261	266
PET A1	48.02	25	50	–	–	–	261	–
PET A2	53.18	-40	25	–		259	–	–
PET A3	49.01	-40	50	254		259	–	–
PET A4	49.82	-40	180	–	257	–	–	–

Infrared spectroscopy of PET fibres

Infrared spectroscopy is a valuable tool for analysis of oxygen functional groups in polymers. Using infrared spectroscopy, Samson et al. [17] have found that the alkali hydrolysis causes scission of PET chains resulting in smaller fragments of ethyleneglycol and terephthalic acid.

Hydrolysis of PET fibres is enhanced at increased humidity above the glass transition temperature T_g. It results in an increased content of carboxylic and alcohol hydroxyl groups and shorter chains due to the reverse esterification [17]. Water diffuses into the amorphous regions of PET, where hydrolysis takes place. The hydrolysis rate depends on the polymer morphology, crystallinity values, relative humidity, and temperature. The process of hydrolysis degradation, often denoted as chemicrystallization, involves changes in density due to the scission of chains in the amorphous regions resulting in short chains with a sufficient mobility, which can crystallize. The effect of chemicrystallization has been detected also upon oxidative degradation. The increase in crystallinity upon degradation significantly affects the tensile strength. It has also been found that the degree of crystallization affects the hydrolysis rate.

ATR (attenuated total reflectance) spectra of the alkali hydrolyzed and laboratory-aged PET fibre samples within the spectral ranges of 3600-2750 cm^{-1} and 1800-650 cm^{-1} are shown in Figures 3 and 4. The bands at 3545 and 3430 cm^{-1}, and the region 3380-3210 cm^{-1} have been assigned to hydroxyl groups of absorbed water, OH stretching of diethyleneglycol end group, and Ar–OH, respectively. The changes in content of hydroxyl groups have been expressed by the ratio of band areas $A_{3545}/(A_{3545} + A_{3430})$. The alkali hydrolyzed samples and the laboratory-aged samples A3 and A4 showed an increase in hydroxyl groups of absorbed water (see Figure 5), which confirms an increased hydrophility of these fibre samples. The changes in content of carboxyl groups have been expressed by the ratio of band areas $A_{1728}/(A_{1728} + A_{1713})$. It is obvious from the results presented in Figure 6 that the content of carboxyl groups has been increased except for the alkali hydrolyzed samples, where the carboxyl content has slightly declined.

Figure 3. ATR spectra of the original and modified PET fibres within the spectral range 3600-2750 cm^{-1}; A: PET, B: PET AHCa, C: PET AHNa, D: PET A1, E: PET A2, F: PET A3, G: PET A4.
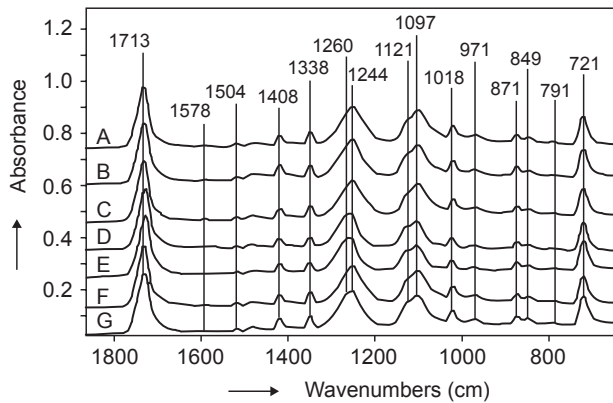

Figure 4. ATR spectra of the original and modified PET fibres within the spectral range 1800-650 cm^{-1}; A: PET, B: PET AHCa, C: PET AHNa, D: PET A1, E: PET A2, F: PET A3. G: PET A4.
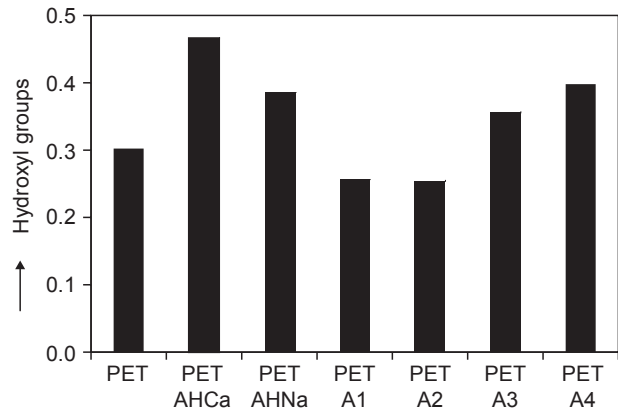

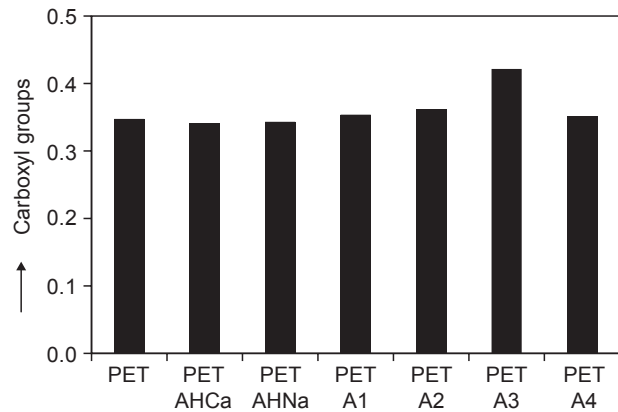Figure 5. Relative abundance of hydroxyl groups in the original and modified PET fibres.

Figure 6. Relative abundance of carboxyl groups in the original and modified PET fibres.

Vibrational spectroscopy is a valuable tool for studying polymer morphology, i.e., determination of the crystalline and amorphous region in PET. Molecular conformational changes play an important role in determination of PET structure. Rodriguez-Cabello et al. [16], e.g., determined the distribution of the *trans*/*gauche* conformers by infrared spectroscopy using the 968 cm^{-1} band intensity of the *trans* isomer (O–CH$_2$ stretching vibration) and the 898 cm^{-1} band intensity of the *gauche* isomer (glycol segment), relative to the 793 cm^{-1} band intensity (CH aromatic deformation mode). Regarding that the bands employed were not well resolved, band separation has been applied. For determination of the content of the *trans* and *gauche* conformation isomers, and thus the crystallinity changes of the PET fibres analyzed in the present work, a two-phase conformation model has been used:

$$p_1\, I_{968}/I_{793} + p_2\, I_{898}/I_{793} = 1 \qquad (1)$$

where p_1 and p_2 are constants [16]. Figure 7 shows the part of an ATR spectrum of the original PET fibres used for separation of the bands assigned to the *trans* and *gauche* conformation isomers. The bands have been
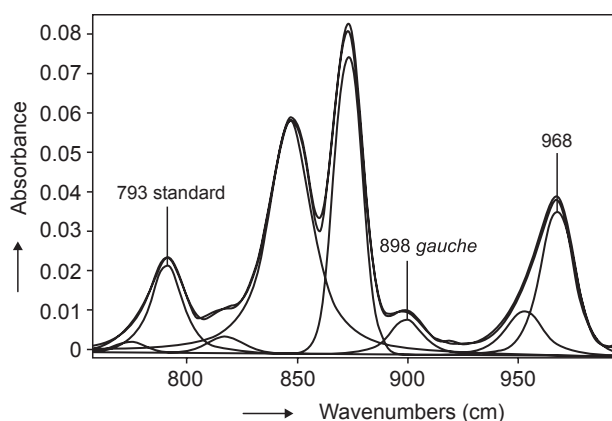
separated using the Voigt function, and the p_1 and p_2 constants in Equation (1) found to be 0.4847 and 0.7484, respectively.

Besides the content of the *trans* and *gauche* isomers in the amorphous region, infrared spectroscopy provides information on the total content of the *trans* conformation isomers (total *trans*) in both crystalline and amorphous regions of the polymer. The DSC results provide the *trans* isomer content in the crystalline fraction only (crystalline *trans*). Subtracting the crystalline *trans* (DSC) from the total *trans* (ATR) will provide the content of the *trans* isomers in the amorphous fraction (amorphous *trans*). Percentages of the individual isomers are given Table 2.

Mechanical properties of PET fibres

Rodrigues-Cabello et al. [16] have found that the content of the *trans* conformation isomers in the crystalline region does not change significantly with increasing temperature, whereas the content of *trans* isomers in the amorphous zone decreases with increasing temperature after reaching the glass transition temperature (T_g = 75-80°C). This conformation transition connected with a loss of orientation of polymeric chains of the amorphous phase is reflected in a macroscopic effect - Young's modulus, which is virtually constant below T_g and then decreases rapidly. Although mechanical behaviour can be controlled by the crystalline zone structure of a polymer, it has been shown that in the case of PET fibres it is influenced by the amorphous phase structure. Similar finding has been done for mechanical behaviour of the degraded PET fibres in the present work. An example of deformation curves of the original (PET), alkali hydrolyzed with Ca(OH)$_2$ (PET AHCa), and laboratory-aged (PET A1) fibres is presented in Figure 8. From shapes of the deformation curves it is evident that for the modified fibres, Young's modulus and maximum stress decrease compared to the original sample, whereas strain increases. Table 2 lists the mechanical parameters of the original and modified PET fibres

Figure 7. Separation of the bands of the trans and gauche conformation isomers in an ATR spectrum of the original PET fibres.

Table 2. Contents of the trans and gauche conformation isomers and mechanical parameters of the original and modified PET fibres.

Sample	crystalline *trans*[a] (%)	total *trans*[b] (%)	*gauche*[c] (%)	amorphous *trans*[d] (%)	Young's modulus E_F (GPa)	maximum stress σ_{max} (MPa)	first failure strain (%)	last failure strain (%)
PET	43.54	85.96	23.52	42.42	10.6 ± 3.1	666.8 ± 30.1	10.79	11.50
PET AHCa	46.32	66.38	22.83	20.06	9.1 ± 0.55	590.2 ± 38.6	11.79	13.90
PET AHNa	41.97	77.32	21.66	35.35	8.8 ± 0.59	586.8 ± 32.8	12.21	14.31
PET A1	48.02	69.46	39.20	21.44	5.1 ± 0.46	426.1 ± 37.8	18.30	18.61
PET A2	53.18	67.01	37.72	13.83	7.1 ± 0.47	459.4 ± 50.0	11.52	13.90
PET A3	49.01	70.01	25.89	21.00	9.3 ± 0.42	620.8 ± 42.1	12.20	12.82
PET A4	49.82	60.23	37.14	10.41	5.0 ± 0.16	510.7 ± 36.3	17.40	19.88

a - DSC, b - FTIR, c - FTIR, d - FTIR total *trans*/DSC *trans*

together with the values of the strain at the first and last failure before fibre breakage. Figure 9 shows the relations between Young's modulus and the content of the *trans* and *gauche* conformation isomers. It is indicated by (Table 2) and Figure 9 that Young's modulus and the stress before fibre failure increase with increasing content of the *trans* isomers in the amorphous fraction of the PET fibres studied, whereas the *gauche* and crystalline *trans* isomers show a reverse trend, in agreement with literature [16]. It follows also from the results that the alkali hydrolyzed fibres and the thermally aged fibre PET A3 have about 90% strength of the original undegraded PET fibre, whereas the thermally aged fibres PET A1, A2, A4 have 65-77 % strength of the original undegraded PET fibre. The degraded PET fibres with a higher strength have higher content of the amorphous *trans* isomers and lower content of the *gauche* isomers. A simplified diagram of the structural changes in the crystalline and amorphous fraction in PET fibres upon aging is depicted in Figure 10.

a)
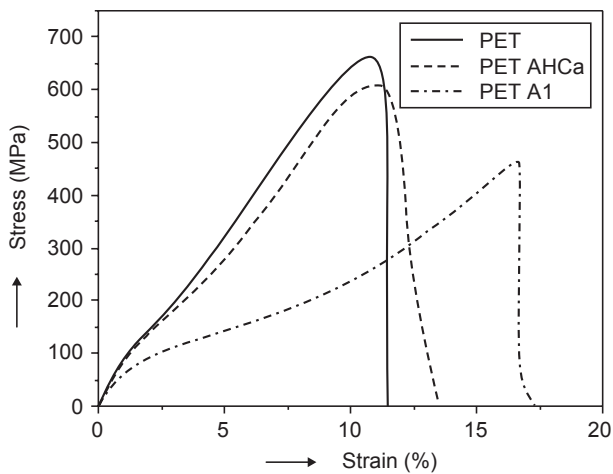
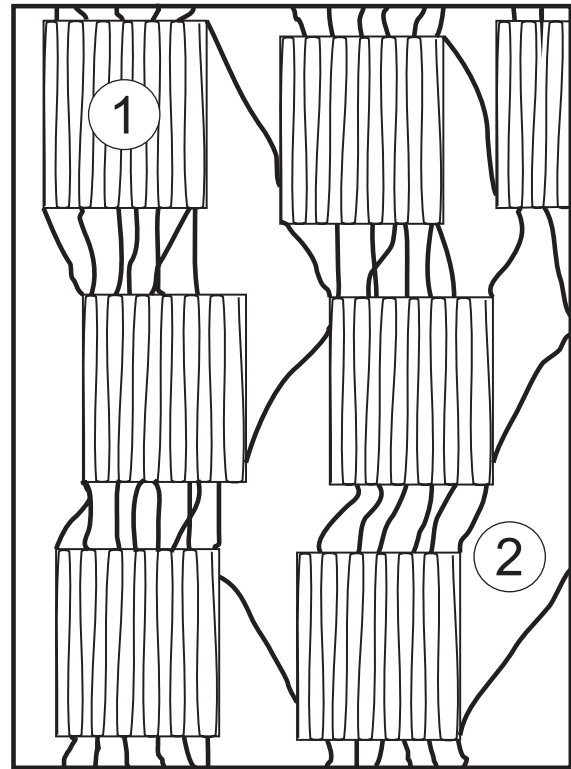Figure 8. Strain-stress deformation curves of the original and selected modified PET fibres.
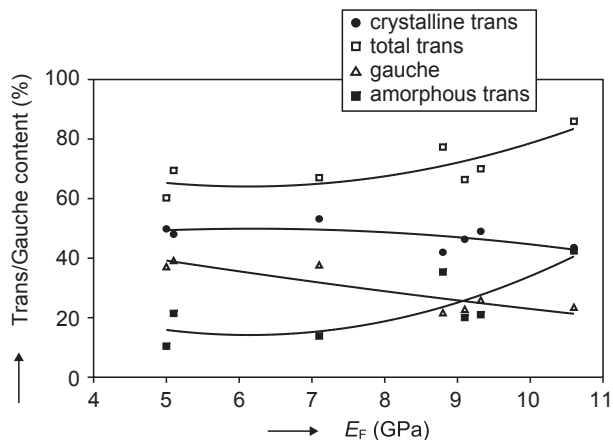
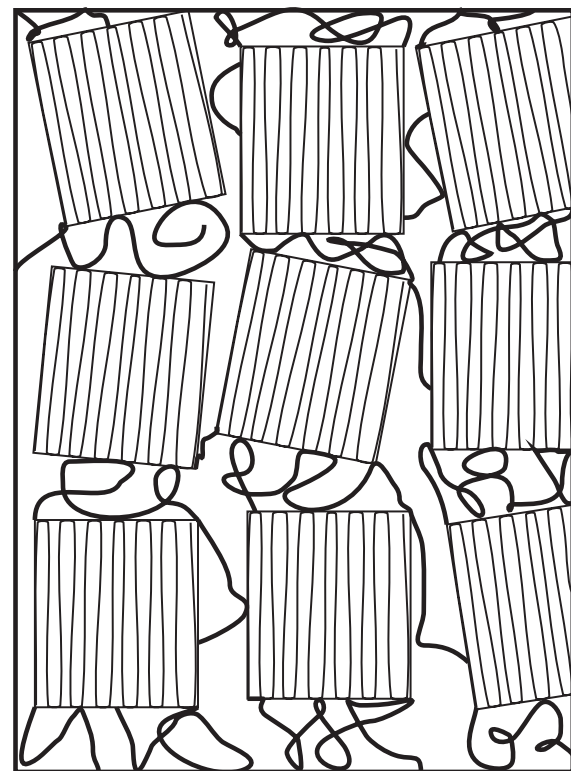
Figure 9. Relations between the Young's modulus and the content of the trans and gauche conformation isomers.

b)

Figure 10. Diagram of the structural changes in the crystalline and amorphous fraction in original a) and modified PET fibre b), 1 - crystalline trans zone, 2 - amorphous trans zone.

Water vapour sorption onto PET fibres

Hydrophobic polymers absorb usually less than 1 wt.% of water. For hydrophobic polymers such as PET, the sorbed water changes their physical properties such as the glass transition temperature, dielectric constant, and Young's modulus [19]. Application of fibres in a composite matrix requires strong adhesion between the fibre and matrix. Changes in the PET fibre surface properties after their alkali hydrolysis and laboratory-aging can be studied by water vapour sorption. Figure 11 shows that the degraded fibres are better water sorbents than the original fibres. This can be explained by an increase in the specific surface of the fibre, and partially by formation of new organic groups (COOH and OH) with a higher affinity to water sorption. Significant correlation has not been found between the structural or mechanical parameters of the PET fibres and the content of water adsorbed on the fibre surface.

Micropore distribution on the surface of the original and alkali hydrolyzed PET fibres was studied by CO_2 sorption (see Figure 12). Micropores with a diameter of 7 nm prevail in the PET fibres. The surface occupied by micropores is 36.56 m^2/g in the original PET fibre, after alkali hydrolysis with NaOH and $Ca(OH)_2$ it has been increased to 37.82 and 45.34 m^2/g, respectively.
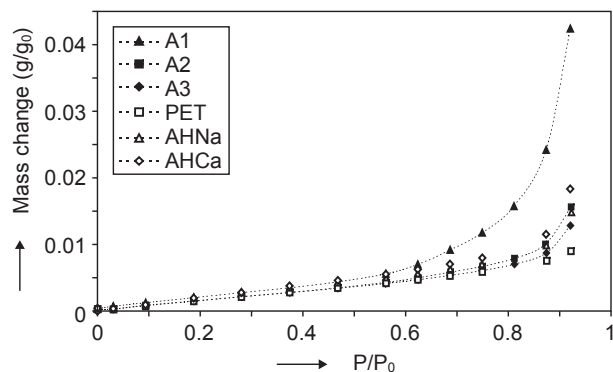

Figure 11. Water vapour sorption isotherms for the original and modified PET fibres.
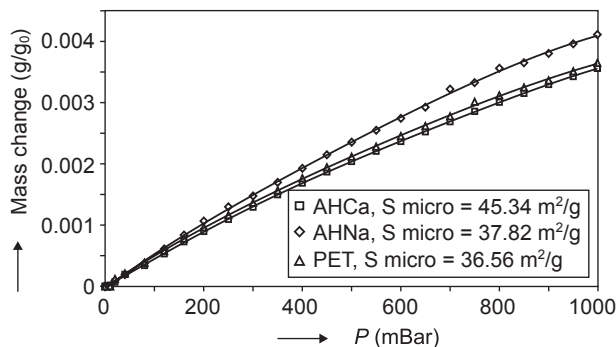

Figure 12. Sorption of CO_2 on the original and alkali hydrolyzed PET fibres, and determination of surface and micropore distribution.

Environmental scanning electron microscopy (ESEM) enables investigation of the surface structure modifications. An increased appearance of defects on the surface of the alkali hydrolyzed and laboratory-aged PET fibres is documented by the ESEM micrographs in Figure 13. The surface defects are not visible on the original PET fibres, whereas small regular cracks are present on the surface of the alkali hydrolyzed PET fibres and irregular defects of a larger size can be found on the aged PET fibres.

Porosity of cement composite

Porosity of the cement composites reinforced with the original and alkali hydrolyzed PET fibres was studied by mercury porosimetry. Pore distribution has been determined for the composites hydrated for 40 days. From Figure 14 it follows that the addition of the alkali hydrolyzed PET fibres decreases porosity compared to the pure cement without micro reinforcement, and that the lowest porosity can be observed for the cement composite reinforced with the PET fibres alkali hydrolyzed with NaOH. It can be assumed that these fibres have the highest adhesion to the cementitious matrix and the ITZ between the fibre and matrix the lowest content of pores. Thus, this composite was expected to show the highest firmness.

Compressive strength of the PET fibre reinforced cement composite

Mechanical properties of the cement composite depend mainly on the content of fibres, their orientation, and also on the quality of load transfer between the reinforcement and matrix. In the case of the compressive experiment, the presence of fibres in this material does not improve significantly its compressive strength. A positive effect of the fibres was observed mainly visually; the samples with fibers disintegrate and stayed relatively compact until high strains (up to strain of about 10 %), only containing number of smaller cracks. Compression stress-strain curves are depicted in Figure 15. Table 3 lists results of the compressive strength calculated from the maximum load before the first marked failure.

Bending test of the PET fibre reinforced cement composite

From the compression diagrams it has followed that the presence of fibres in the cement material does not cause significant changes in the compressive strength. The presence of PET fibres, however, markedly affects flexural strength. Figure 16 presents flexural load-deflection curves for pure cement and the cement
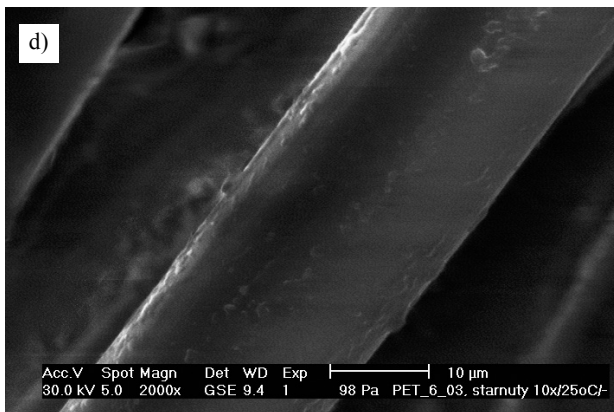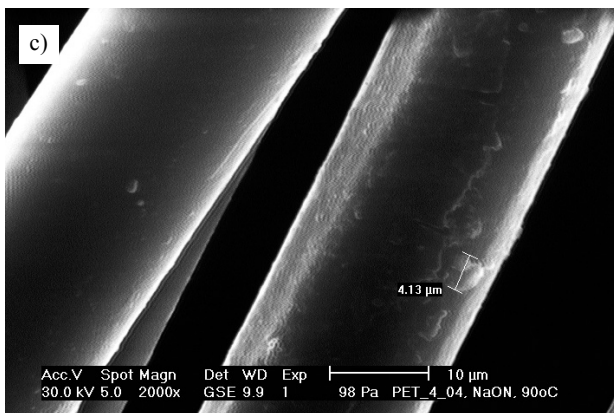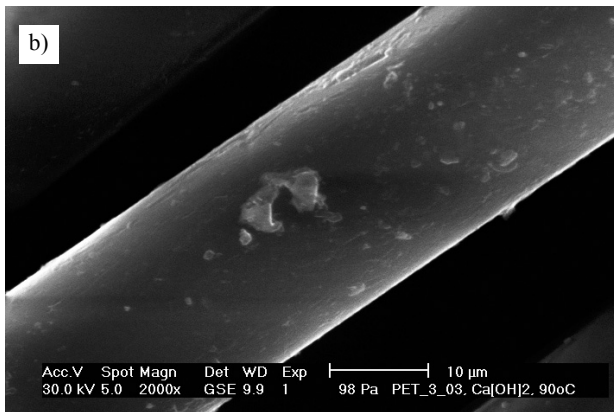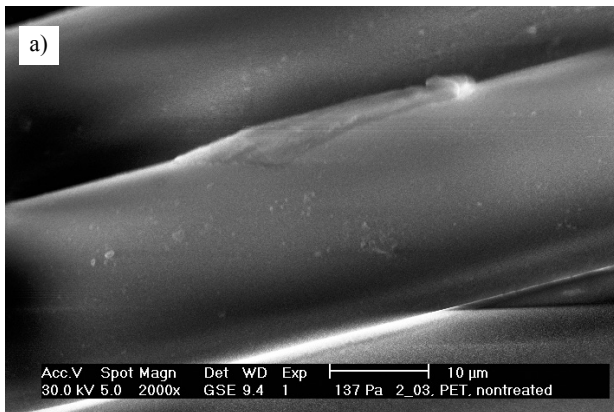
composite with the original PET fibres. The two curves are quite different. The curve characterizing the pure cement paste predicates of linear brittle behaviour. The other curve is typical for cement composites. It can be divided into three regions characterized by two load values. The critical load F^* is a load at the stage when first cracks appear. The region I is characterized by relatively elastic behaviour before the appearance of first cracks, where mainly the cementitious matrix contributes to the load capacity of the composite. Other maxima within the region II between F^* and F_{max} indicate secondary crack occurrence. The peak load F_{max} can
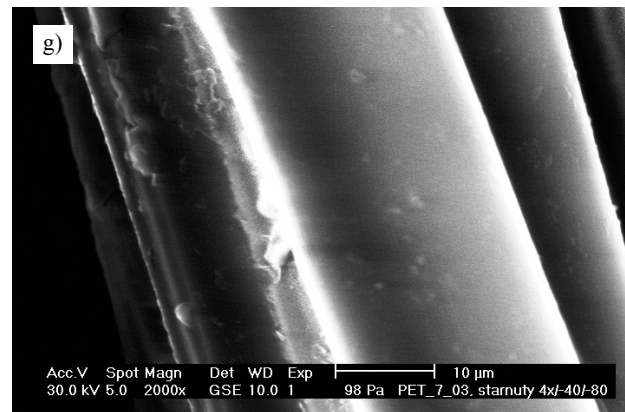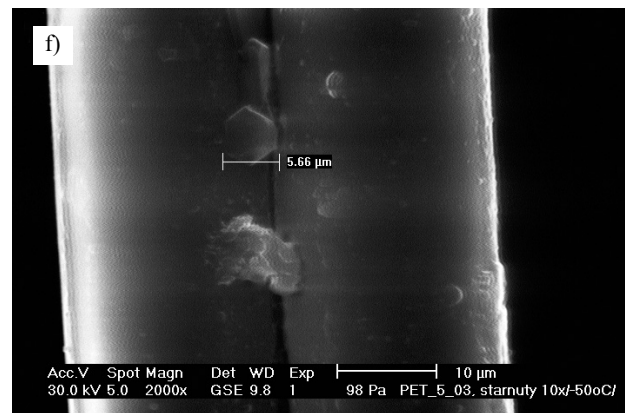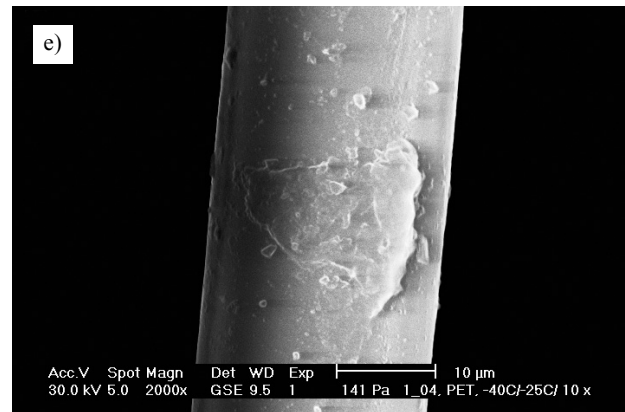
Figure 13. ESEM micrographs of the surface of the original and modified PET fibres; a) PET, b) PET AHCa, c) PET AHNa, d) PET A1, e) PET A2, f) PET A3. g) PET A4.

be interpreted as the highest failure force and the region II is the inelastic range until fracture, where only fibres carry tensile stresses. After the peak load F_{max} (region III), the mechanical behaviour is mostly due to the presence of fibres in the composite. No sudden failure but a continuous fall of the load has been observed. This behaviour underlines the major role of the debonding process in the ruin of the material [6]. Figure 17 illustrates the final stage of the three-point bending test, where all fibres break.
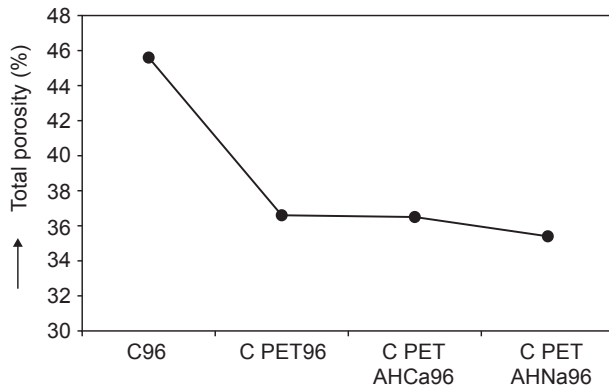

Figure 14. Porosity of pure cement and PET-cement composites reinforced with the original and alkali hydrolyzed PET fibres.
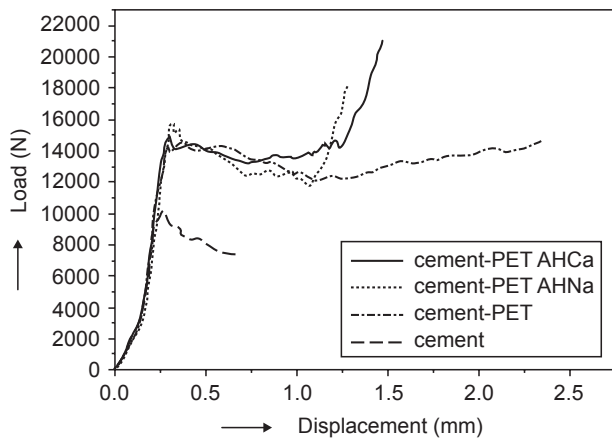

Figure 15. Compression stress-strain curves for pure cement and PET-cement composites with the original and alkali hydrolyzed PET fibres.

The results of the bending test expressed by the flexural modulus E_C and flexural strength $\sigma_{b,max}$ are presented in Table 3. It is evident that the PET fibre addition to cement has increased its flexural strength and modulus. As obvious from Figure 18, the flexural modulus of a PET-cement composite is linearly proportional to Young's modulus of a respective PET fibre with various aging degree obtained by alkali hydrolysis or temperature cycles, with the highest modulus observed for the composite reinforced with the original PET fibres. On the other hand, the dependence of the flexu-
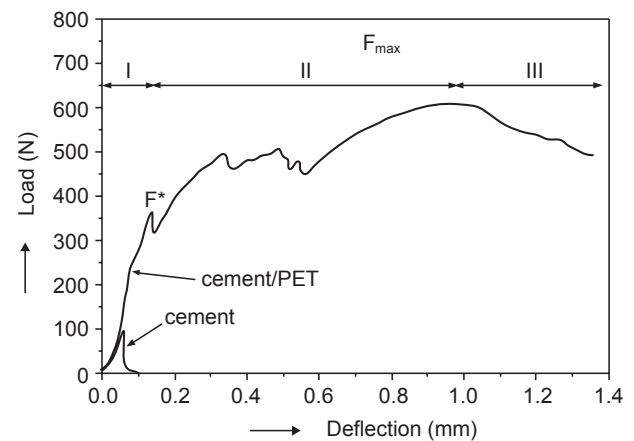

Figure 16. Flexural load-deflection curves for pure cement and PET-cement composite with the original PET fibres.
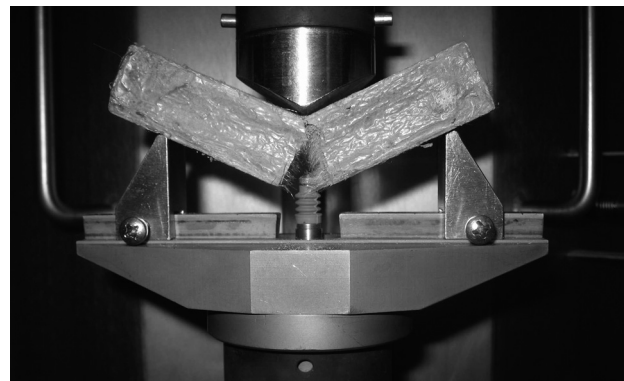

Figure 17. Three-point bending test.

Table 3. Mechanical properties of various PET-cement composites after 40 days of curing.

Sample	Compressive strength $\sigma_{c,max}$ (MPa)	Flexural strength $\sigma_{b,max}$ (MPa)	Flexural modulus E_C (GPa)
cement	16.0 ± 4.8	1.0 ± 0.4	1.01
cement-PET	19.6 ± 0.6	9.1 ± 0.3	3.43
cement-PET AHCa	22.3 ± 4.3	7.3 ± 0.5	2.90
cement-PET AHNa	24.8 ± 5.6	11.6 ± 0.7	2.81
cement-PET A1	n.d.	6.6 ± 0.5	1.32
cement-PET A2	n.d.	4.1 ± 0.4	2.27
cement-PET A3	n.d.	10.0 ± 0.6	2.81
cement-PET A4	n.d.	5.9 ± 0.4	1.62

n.d. - not determined

ral strength of various PET-cement composites on tensile strength of respective PET fibres see Figure 19 is ambiguous. The composite reinforced with the fibres hydrolyzed with NaOH has the highest flexural strength (127 % of the strength of the composite with the original PET fibres). The composite reinforced with these fibres is characterized with a very low porosity, and thus very good adhesion to the cementitious matrix in the ITZ region between the fibre and matrix. Also the composite with the thermally aged fibres A3 has higher strength compared to the composite with the original PET fibres (110 %). The composite with the PET fibres hydrolyzed with $Ca(OH)_2$ has an 80% strength compared to the composite with the original PET fibres. Other composites with the thermally aged fibres PET A1, PET A2, and PET A4 show 73 %, 45 % and 65 % strengths. It follows from the results that the composite strength depends mainly on the strength of the PET fibres.

CONCLUSION

The results can be summarised as follows:

● Chemical and thermal degradation of PET fibres used as micro-reinforcement in a cementitious matrix have been studied. Before addition to the cementitious matrix, the fibres were either alkali hydrolyzed with NaOH or $Ca(OH)_2$ under elevated temperature, or laboratory-aged using various temperature cycles. This treatment should have simulated aging of PET fibres in concrete in the course of its hydration a weathering.

● Infrared spectroscopy has revealed that the alkali hydrolysis induces scission of polymeric chains into smaller fragments of ethyleneglycol and terephthalic acid, and increases the content of hydroxyl groups on the PET fibre surface. The thermal aging of PET fibres has increased the content of carboxyl groups and in some cases also hydroxyl groups.
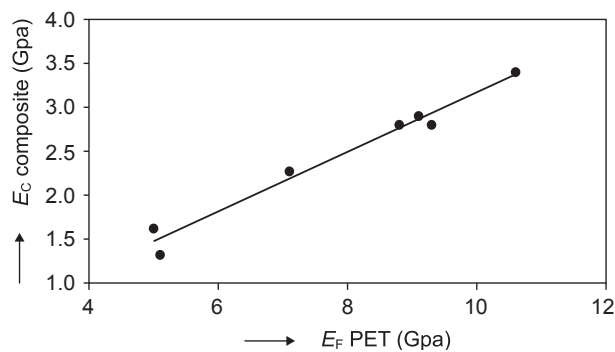
● DSC in combination with infrared spectroscopy was used for determination of the degree of crystallization and content of the *trans* and *gauche* conformation isomers in the original and modified PET fibres. The PET fibre crystallinity determined using DSC is lower in all aged samples except for the sample alkali hydrolyzed with NaOH. For all modified samples, the total content of the total and amorphous *trans* isomers after the degradation has decreased compared to the original PET fibres. The content of *gauche* isomers has increased in the thermally aged samples, whereas a moderate decrease has been observed for the alkali hydrolyzed samples.

● Young's modulus of the degraded PET fibres and the stress before breakage increases with increasing content of the *trans* isomers in the amorphous fraction of PET fibres, whereas the *gauche* and crystalline *trans* contents follow a reverse trend.

● The degraded PET fibres with a higher content of the amorphous *trans* isomers and lower content of the *gauche* isomers, namely the alkali hydrolyzed fibres, have about 90% strength of the original fibre. The fibres aged by the temperature cycles with about 65-77 % strength of the original PET fibre contain a higher amorphous fraction.

● The fibres attacked by $Ca(OH)_2$ and NaOH show a higher ability for H_2O sorption than the original fibre thanks to an increased fibre surface and formation of hydroxyl and carboxyl groups on the fibre surface. Similar trend has been observed for the content of micropores determined by carbon dioxide sorption.

● Porosity of the PET-cement composite decreases with the PET fibre addition and with modification of their surface by alkali hydrolysis.

● The three-point bending has shown that a 2 wt.% admixture of PET fibres in cement markedly increases its maximum flexural strength and modulus. The highest strength has been obtained for the cement composite reinforced with the fibres alkali hydrolyzed with NaOH. It can be assumed that the chemi-

Figure 18. Dependence of flexural modulus of various PET-cement composites on Young's modulus of respective PET fibres.
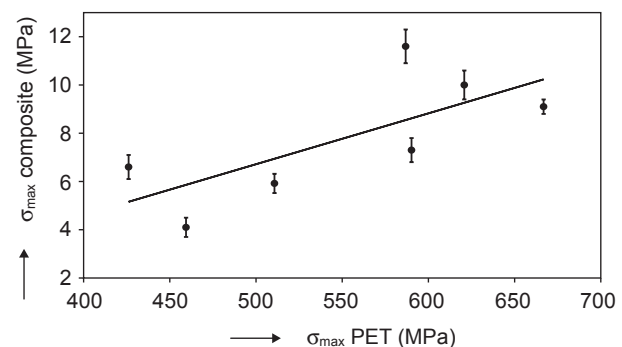

Figure 19. Dependence of the flexural strength of various PET-cement composites on the tensile strength of respective PET fibres.

cal degradation increases adhesion of the fibre to the cementitious matrix in the interfacial transition zone, and thus improves mechanical properties of the PET fibre reinforced cement composite. It is expected that this easy chemical modification of the PET fibre surface will provide very sturdy while cheap concretes reinforced with recycled polymeric fibres.

Acknowledgement

References

1. Silva T., Betioli A. M., Gleize P. J. P., Roman H. R., Gomez L. A., Ribeiro J. L. D.: Cem. Concr. Res. *35*, 1741 (2005).
2. Ochi T., Okubo S., Fukui K.: Cem. Concr. Res. *29*, 448 (2007).
3. MacVicar R., Matuana L. M., Balatinecz J. J.: Cem.Concr. Res. *21*, 189 (1999).
4. Peled A., Bentur A., Composites *A 34*, 107 (2003).
5. Ramakrishna G., Sundararajan T., Cem.Concr.Res. *27*, 575 (2005).
6. Sedan D., Pagnoui C., Smith A., Chotard T.: J. Europ. Ceram. Soc. *28*, 183 (2008).
7. Pinchin D. J., Tabor D.: Cem.Concr.Res. *8*, 139 (1978).
8. Pera J., Ambroise J., Oriol M., Advn. Cem. Bas Mat. *6*, 116 (1997).
9. Li V. C., Backer S., Cem.Concr.Comp. *12*, 29 (1990).
10. Zheng Z., Feldman D.: Prog. Polym. Sci. 20, 1850 (1995).
11. Kokayashi K, Cho R.: Cem.Concr.Comp. *3*, 19 (1981).
12. Machovič V., Kopecký L., Němeček J., Kolář F., Svítilová J., Bittnar Z., Andertová J.: Ceramics-Silikáty *52*, 54 (2008).
13. Garces P., Fraile J, Vilaplana-Ortego E., Cazorla-Amoros D., Alcocel E. G., Andisón L. G.: Cem.Concr.Res. *35*, 324 (2005).
14. Li G. Y., Wang P. M., Zhao X.: Carbon *43*, 1239 (2005).
15. Wang Y., Backer S., Li V. C.: J. Mater. Sci. *22*, 4281(1987).
16. Rodriguez-Cabello J. C., Santos J., Merino J. C., Pastor J. M.: J. Polym. Sci. *34*, 1243 (1996).
17. Sammon Ch., Yarwood J., Everall N.: Polym. Degrad. Stab. *67*, 149 (2000).
18. Ward I.M.: Chem Ind. *605*, (1956).
19. Fukuda M., Kawai H., Yagi N., Kimura O., Ohta T.: Polymer *31*, 295 (1990).

VLIV STÁRNUTÍ PET VLÁKEN NA MECHANICKÉ VLASTNOSTI CEMENTOVÉHO KOMPOZITU VYZTUŽENÉHO PET VLÁKNY

VLADIMÍR MACHOVIČ*,***, JANA ANDERTOVÁ*, LUBOMÍR KOPECKÝ**, MARTIN ČERNÝ***, LENKA BORECKÁ***, OLDŘIC PŘIBYL***, FRANTIŠEK KOLÁŘ***, JAROSLAVA SVÍTILOVÁ***

*Vysoká škola chemicko-technologická v Praze, Technická 5, 166 28, Praha 6
**Fakulta stavební ČVUT, Thákurova 7, 166 29 Praha 6
***Ústav struktury a mechaniky hornin AV ČR, v.v.i., V Holešovičkách 41, 182 09 Praha 8

Polyetylenteraftalátová (PET) vlákna byla použita jako rozptýlená mikrovýztuž v cementové matrici. Mikrovýztuž ve vláknobetonech absorbuje tahová namáhání a brání vzniku mikrotrhlin vznikajících při smršťování betonu. Tato práce je zaměřena na studium vlivu stárnutí PET vláken alkalickou hydrolýzou a pomocí teplotních cyklů na pevnost cementového kompozitu v tlaku a ohybu. Pomocí DSC, infračervené spektroskopie a sorpce vodní parou a byly charakterizovány chemické změny PET vláken po jejich degradaci a jejich vliv na mechanické vlastnosti PET vláken a výsledného kompozitu PET-cement. Bylo nalezeno, že pevnost kompozitu v ohybu se zvýšila po alkalické hydrolýze PET vláken hydroxidem sodným.